Supplementary Information†

Entropy-mediated lattice strain in a Ruddlesden–Popper perovskite oxide for highly active and bifunctional oxygen electrocatalysis

Taimoor Raza,[a] Sining Yun,[a,*] Naveed Mushtaq,[b] Muhammad Akbar,[c] Abdullah Nasir,[a] Yanbei Liu,[a] Muhammad Qadeer,[a] Rizwan Raza,[d]

[a] Functional Materials Laboratory (FML), School of Materials Science and Engineering, Xi'an University of Architecture and Technology, Xi'an, Shaanxi, 710055, China
[b] School of Physics, Electronics and Intelligent Manufacturing, Huaihua University, Huaihua 418000, China
[c] Institute of Microelectronics and Integrated Circuits, School of Microelectronics, Hubei University, Wuhan, Hubei 430062, China
[d] Clean Energy Research Lab (CERL), Department of Physics, Comsats University Islamabad, Lahore Campus, Pakistan.

*Corresponding author
E-mail: alexsyun1974@aliyun.com; yunsining@xauat.edu.cn

Supplementary Information Include:

Equation: S1–S5

Table S1–S4

Fig. S1–S10

Mixed entropy (ΔS_{mix}) calculation

The mixed entropy for RP perovskite is calculated by using the formula for configurational entropy,[1, 2]

$$\Delta S_{\text{mix}} = -R\left[\left(2\sum_{a=1}^{n} x_a \ln x_a\right)_{\text{A-site}} + \left(\sum_{b=1}^{n} x_b \ln x_b\right)_{\text{B-site}}\right] \quad (S1)$$

HELNOs with an equimolar A-site number of different cations $(La_{0.2}Ca_{0.2}Sr_{0.2}Sm_{0.2}Pr_{0.2})_2$. The A-site in $A_2BO_{4+\delta}$ requires 2.0 atoms per formula unit. Therefore, the mole fraction for each A-site cation is

$$x_a = \frac{\text{individual cation atoms}}{\text{total A-site atoms}} = \frac{0.4}{2.0} = 0.2$$

While the B-site entropy contribution is solely by Ni, so $x_b = 1$. Putting both values in the equation *S*1, we get

$$\Delta S_{\text{mix}} = -R\left[\left(2\sum_{a=1}^{5} 0.2 \ln 0.2\right)_{\text{A-site}} + \left(\sum_{b=1}^{1} 1 \ln 1\right)_{\text{B-site}}\right] \quad (S2)$$

$$\Delta S_{\text{mix}} = -R[2(5(0.2 \ln 0.2))_{\text{A-site}} + (1 \ln 1)_{\text{B-site}}]$$

$$\Delta S_{\text{mix}} = -R[2(5(-0.321888))_{\text{A-site}} + (0)_{\text{B-site}}]$$

$$\Delta S_{\text{mix}} = -R[2(5(-0.321888)]$$

$$\Delta S_{\text{mix}} = -R[2(-1.6094)]$$

$$\Delta S_{\text{mix}} = 3.22R \quad (S3)$$

Goldschmidt tolerance factor (*t*) calculation

The Goldschmidt tolerance factor (*t*) for mixed entropy is calculated by using following values provided in (Table S1),[3, 4]

Table S1 Element and their corresponding oxidation state, coordination number (CN) and cationic radii (r_c)

Element	State	CN	r_c [Å]
La	3^+	12	1.36
Sr	2^+	12	1.44
Ca	2^+	12	1.34
Pr	3^+, 4^+	8	1.04*
Sm	3^+	12	1.24
Ni	2^+, 3^+	6	0.69, 0.56^{LS}, 0.6^{HS*}
O	2^-	6	1.4

LS (low spin), **HS** (high spin), ***** = Average cation value

First, we find average ionic radius at A-site = Avg r_A= (1.36+1.44+1.34+1.043+1.24)/5

$$\text{Avg } r_A = 1.28$$

Putting values in equation

$$t = \frac{1.28 + 1.4}{\sqrt{2}(0.61 + 1.4)} \qquad (S4)$$

$$t = \frac{2.68}{2.82} = 0.95 \qquad (S5)$$

Materials characterization

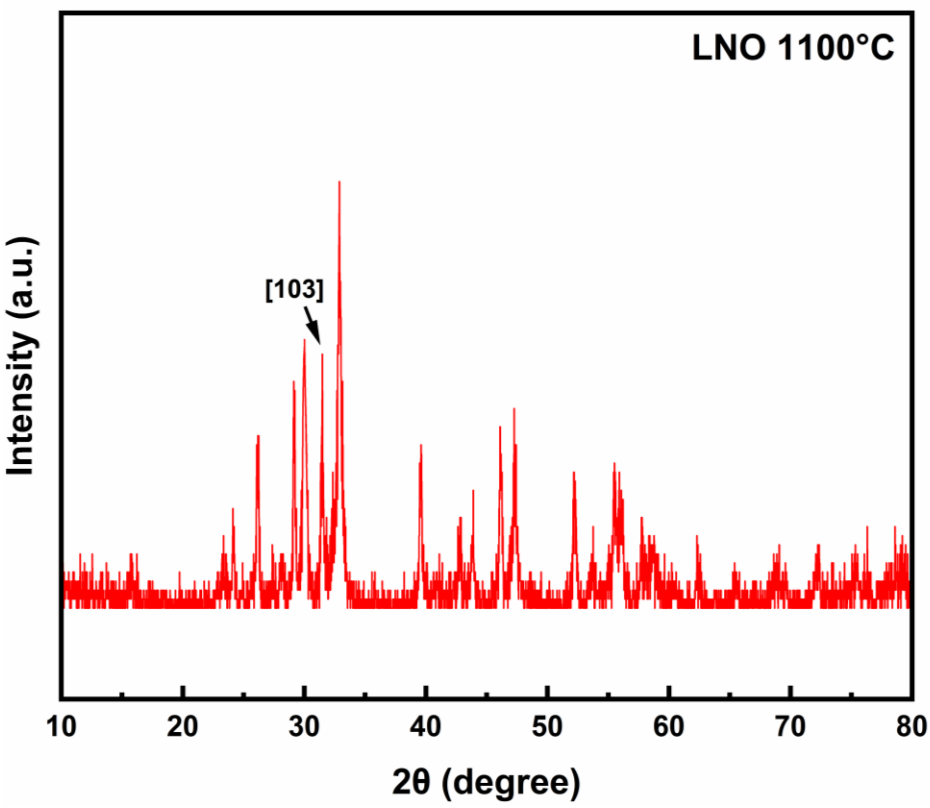

Fig. S1 XRD pattern of LNO calcinated at 1100 ℃

Table S2 The obtained values of lattice parameters, micro strain, residual internal stress and dislocation density of primary facet (103).

Name	2θ (°)	θ (°)	a (Å)	c (Å)	V $(Å)^3$	β (radian)	Dx (g/cm^3)	δ $(Lines/m^2)$	ϵ (%)
LNO	31.414	15.707	3.855	12.652	188.02	0.002093	7.07	1.94	0.19
HELNO	31.934	15.967	3.8198	12.3518	180.22	0.003292	6.37	4.78	0.29

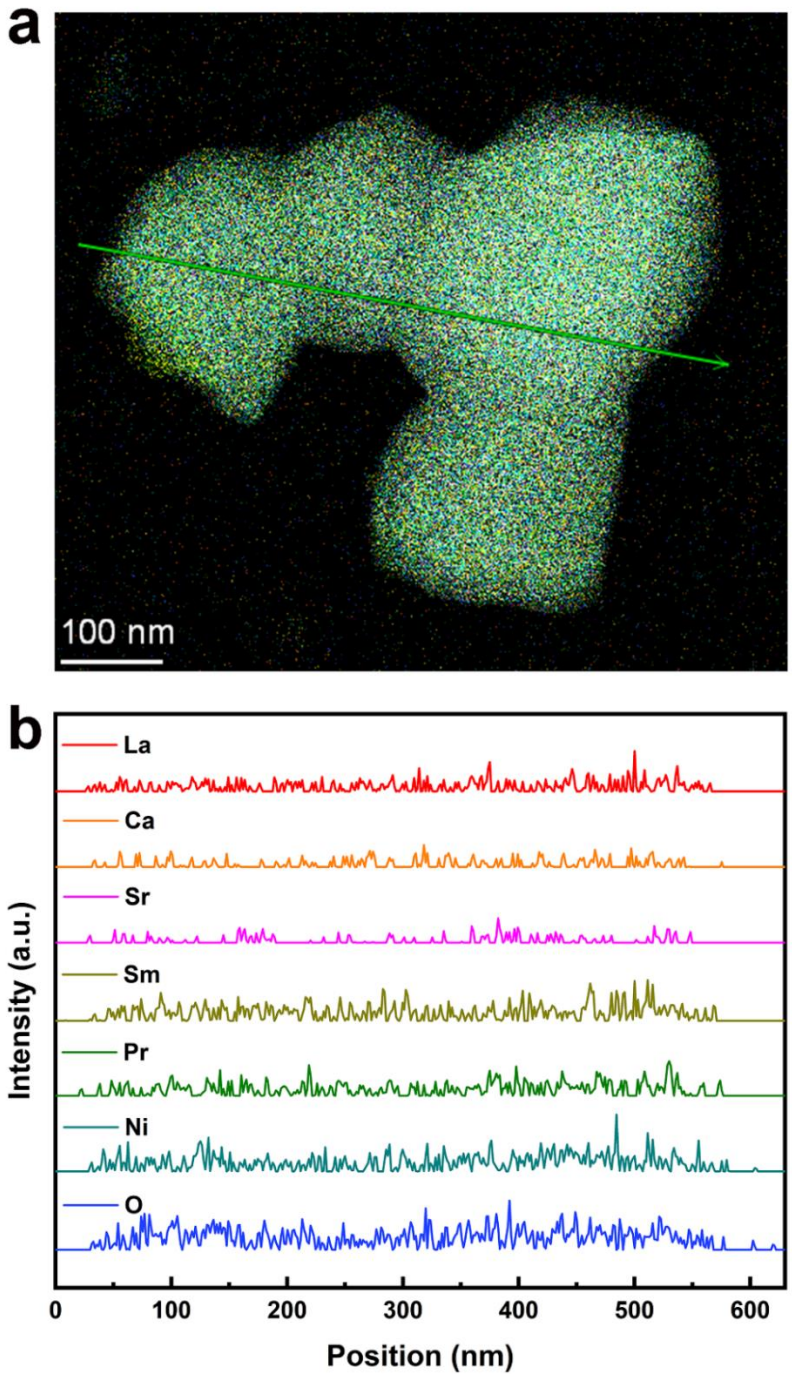

Fig. S2 (a) STEM-EELS image of magnified HELNO with line scanning profile. (b) Intensity concentration line profiles count of La, Ca, Sr, Sm, Pr, Ni, O along the line drawn.

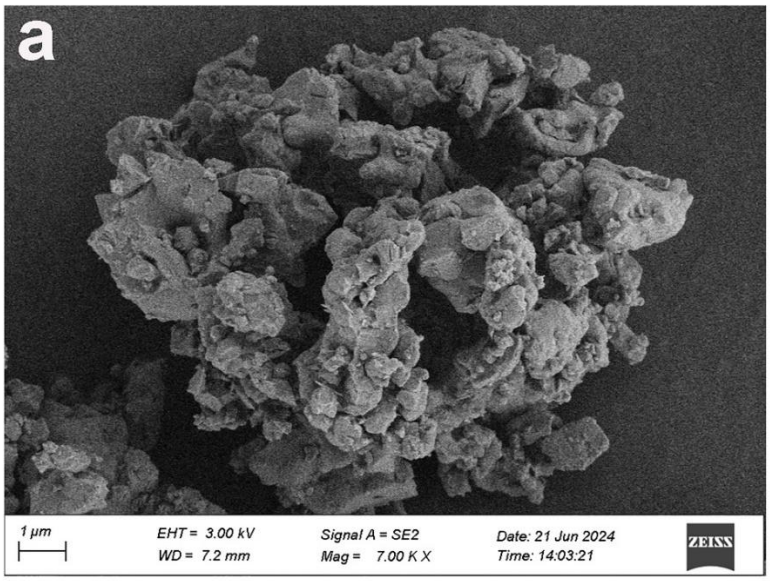

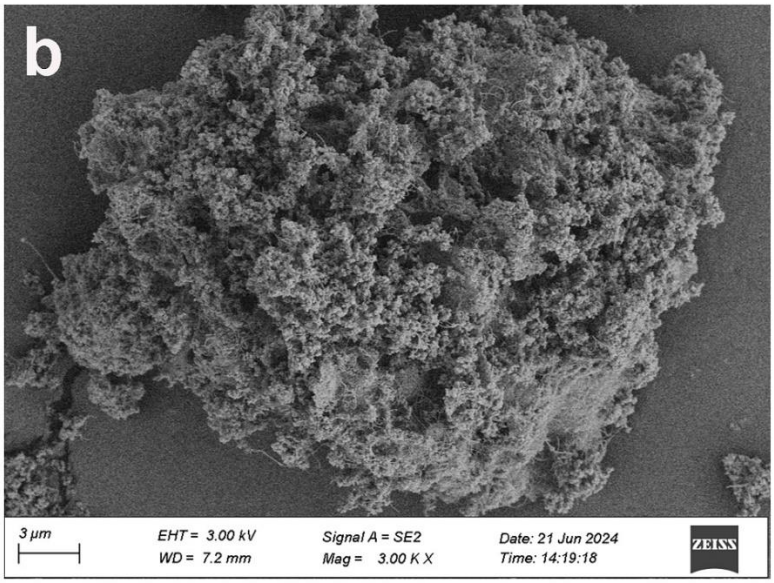

Fig. S3 Surface morphology observation of: (a) SEM image of as prepared HELNO crystallites clusters and agglomerates of different sizes, (b) SEM image of as prepared LNO with crystallite clusters.

Table S3 FTIR absorption band positions corresponding to metal-oxygen (Ni–O) stretching or lattice modes.

Name	V_1 (cm^{-1})	V_2 (cm^{-1})	V_{avg} (cm^{-1})	$K_1 \times 10^5$ (dyne/cm)	$K_2 \times 10^5$ (dyne/cm)	$K_{avg} \times 10^5$ (dyne/cm)
LNO	855	730	792.5	5.41	3.94	4.68
HELNO	854	700	777	5.39	3.62	4.51

Table S4 EIS simulated data for HELNO and LNO cathodes.

Fuel Cells	T (°C)	R_0 $\Omega\ cm^2$	R_1 $\Omega\ cm^2$	R_2 $\Omega\ cm^2$	R_p $\Omega\ cm^2$
	650	0.061	0.005	0.218	0.26
	600	0.109	0.017	0.252	0.27
HELNO	550	0.124	0.026	0.257	0.28
	500	0.112	0.056	0.662	0.72
	450	0.084	0.118	1.068	1.18
LNO	650	0.069	0.024	0.44	0.46

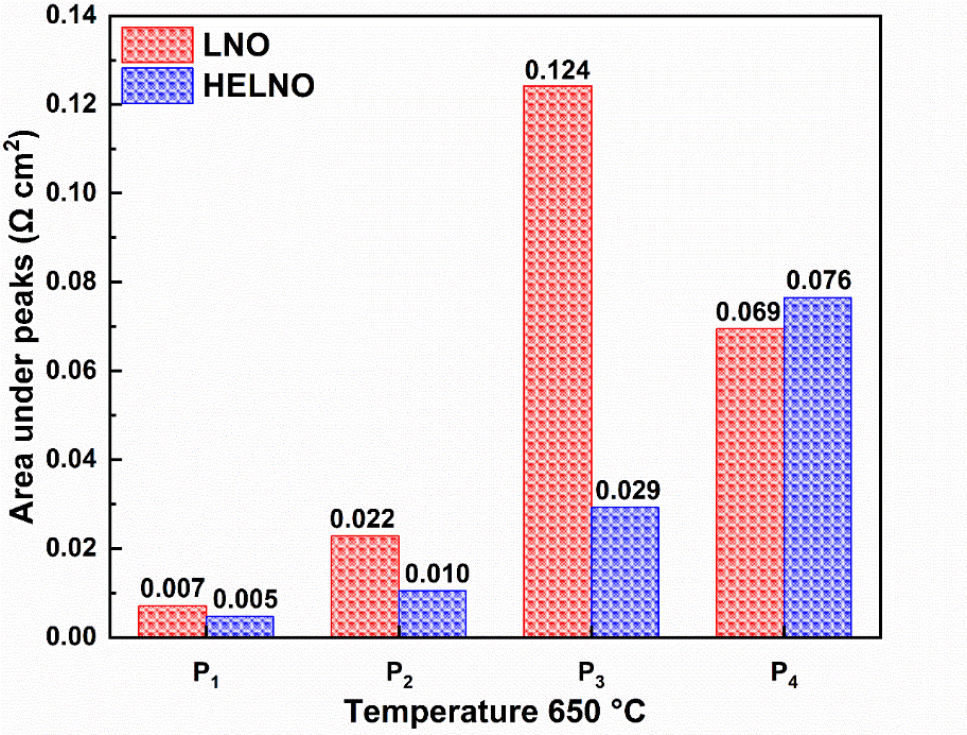

Fig. S4 The DRT analysis area under the peaks, representing sub-processes involved to demonstrate effects of electrochemical reactions in H_2/Air atmosphere of LNO and HELNO.

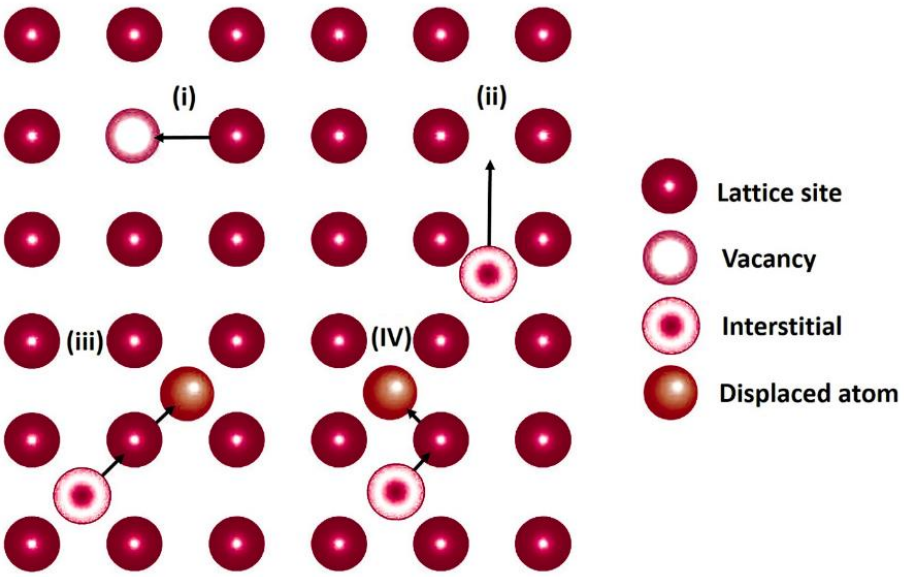

Fig. S5 Diffusion mechanisms of oxygen ions in RP perovskites under SOFC operation. There are four types of oxygen diffusions, (i) diffusion through vacancy, (ii) interstitial diffusion, (iii) interstitial diffusion (collinear), (iv) interstitial diffusion (non-collinear).

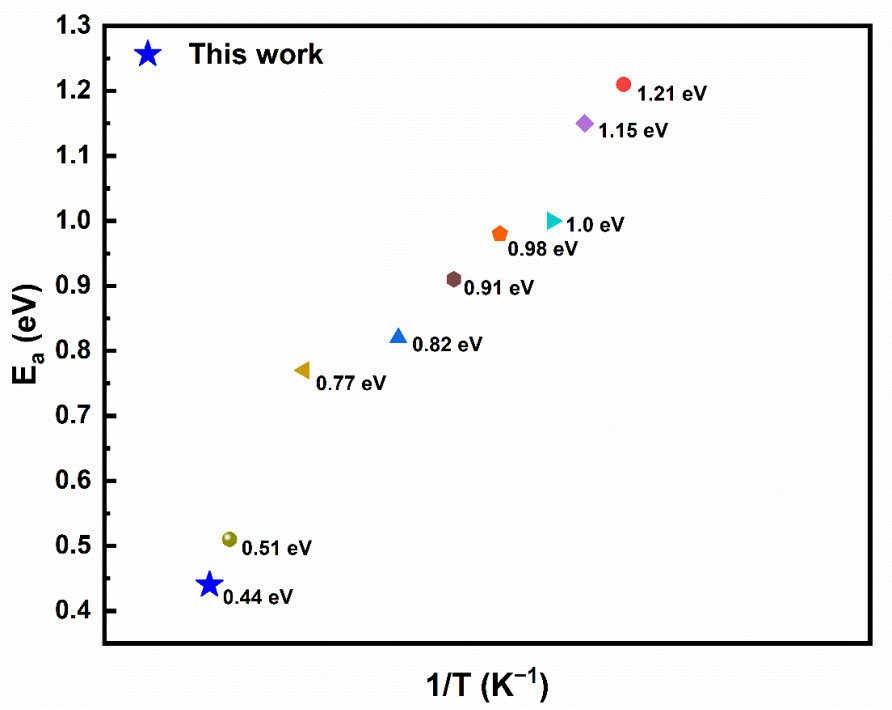

Fig. S6 Calculated HELNO activation energy (E_a) and its comparison with some landmark recent studies in the literature.[5-10]

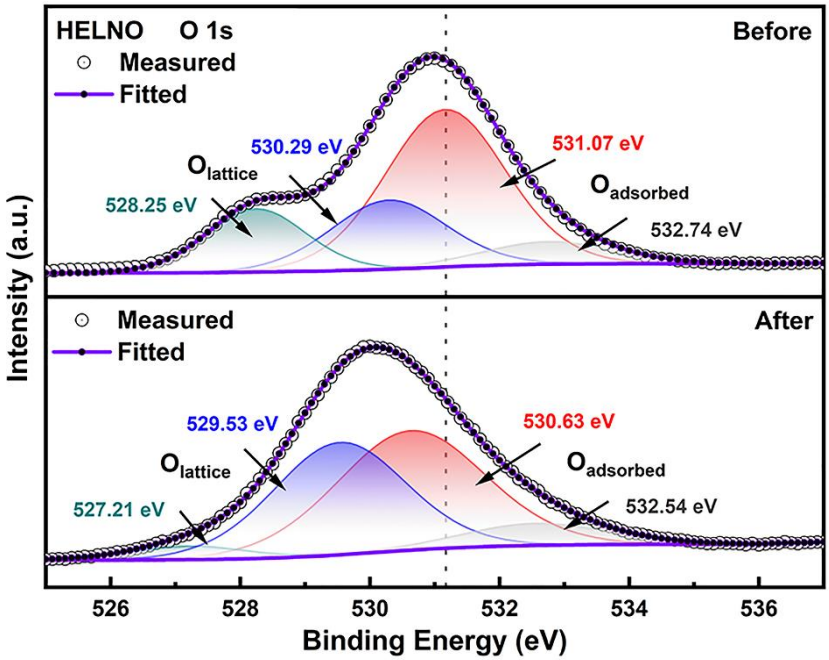

Fig. S7 XPS deconvolution of O 1s for HELNO before and after 100 h stability.

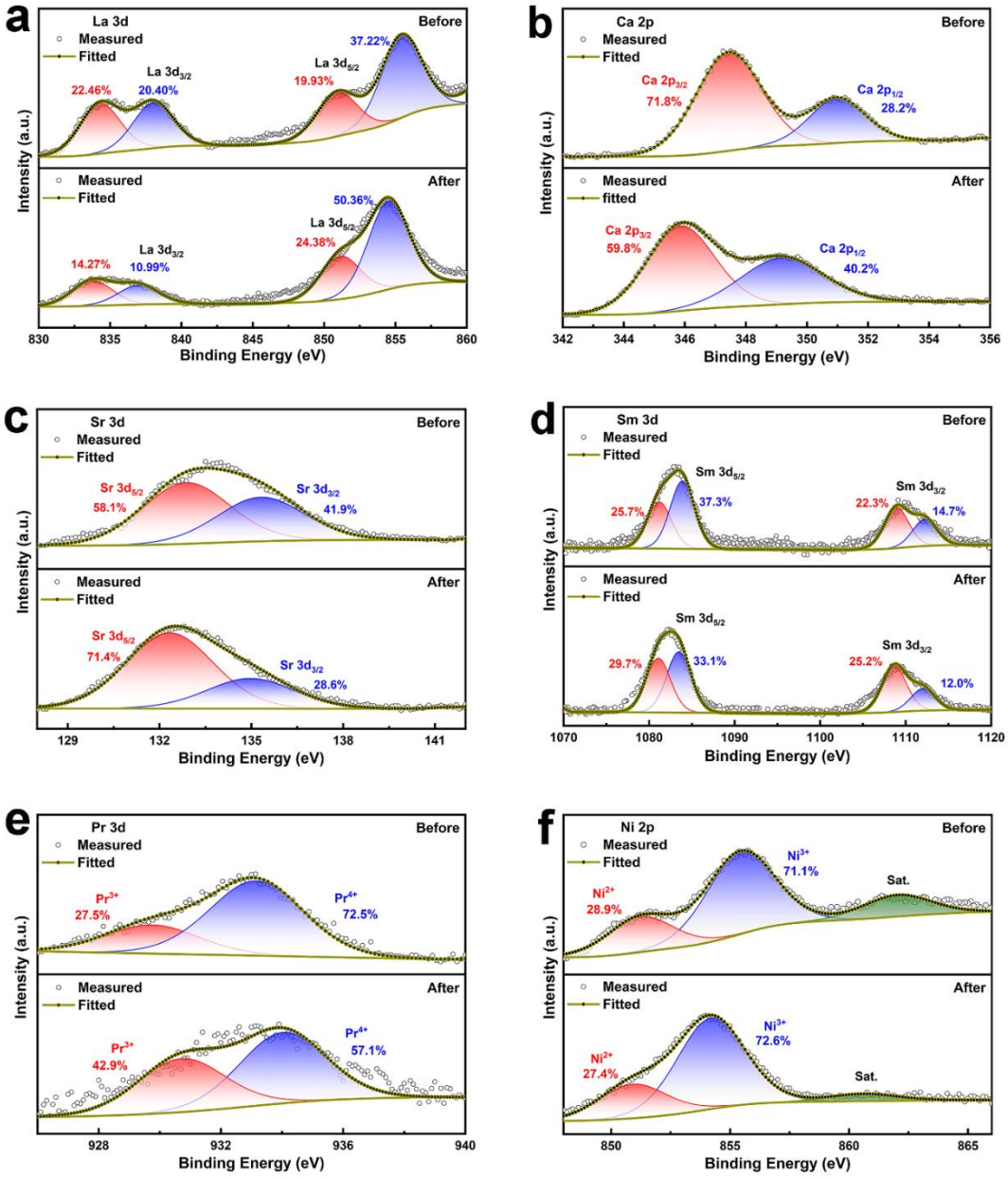

Fig. S8 HELNO XPS spectra of before and after 100 h stability. (a–f) La, Ca, Sr, Sm, Pr and Ni, respectively.

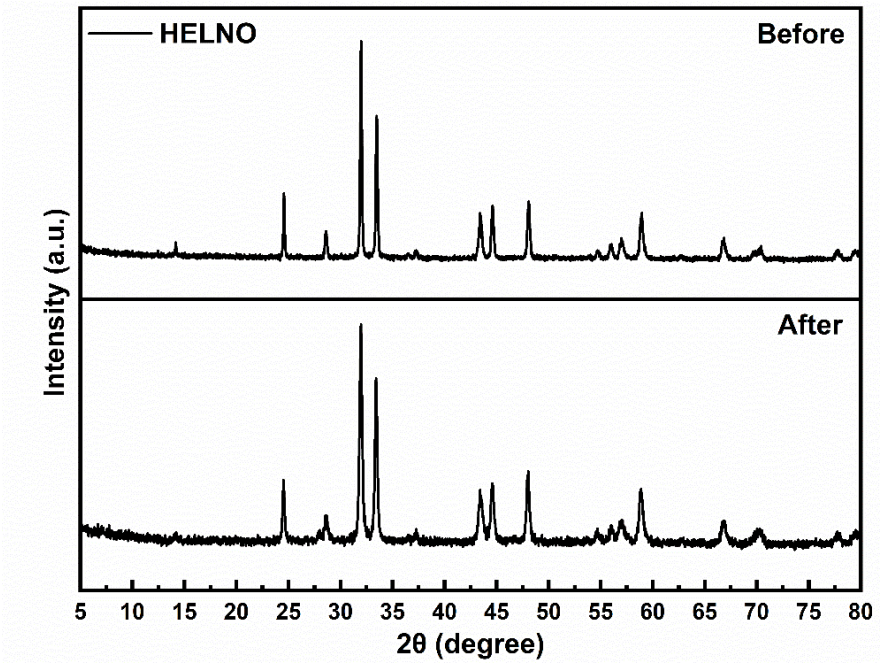

Fig. S9 XRD patterns of HELNO before and after OER treatment. After stability testing, peaks show low intensity and broadening, indicating cations leaching on the surface.

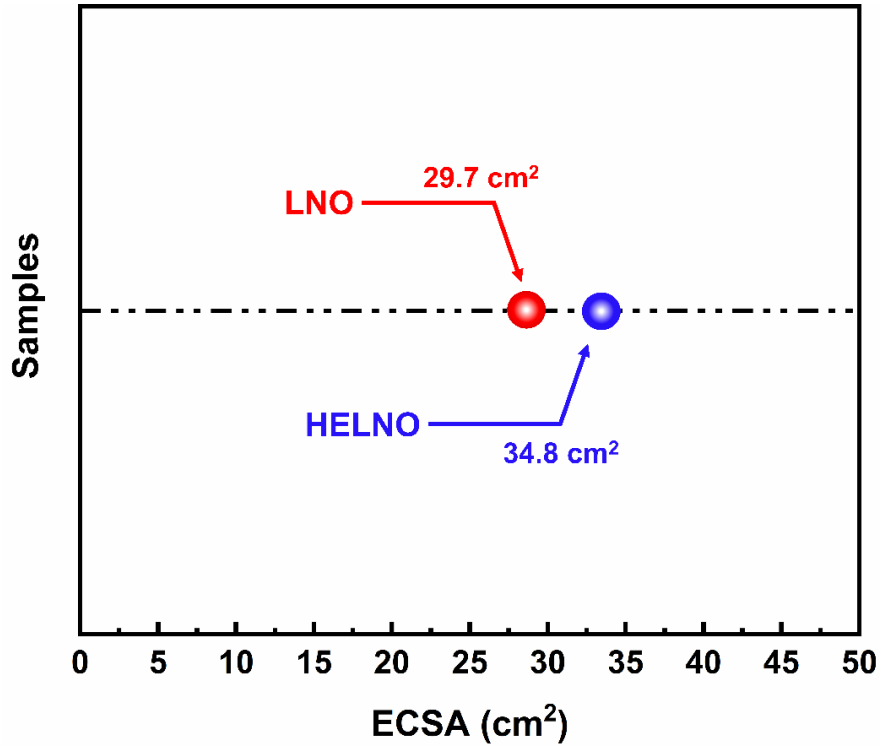

Fig. S10 ECSA values of LNO and HELNO determining the active sites on surface in the field of OER.

References

1. B. Ye, T. Wen, K. Huang, C. Wang and Y. Chu, *J. Am. Ceram. Soc.*, 2020, **103**, 2244-2251.
2. P. A. Krawczyk, M. Jurczyszyn, J. Pawlak, W. Salamon, P. Baran, A. Kmita, Ł. Gondek, M. Sikora, C. Kapusta, T. Strączek, J. Wyrwa and A. Żywczak, *ACS Appl. Electron. Mater.*, 2020, **2**, 3211-3220.
3. R. D. Shannon, *Acta Crystallogr. A*, 1976, **32**, 751-767.
4. A. Sarkar, R. Djenadic, D. Wang, C. Hein, R. Kautenburger, O. Clemens and H. Hahn, *J. Eur. Ceram. Soc.*, 2018, **38**, 2318-2327.
5. W. Zhang, H. Wang, K. Guan, Z. Wei, X. Zhang, J. Meng, X. Liu and J. Meng, *ACS Appl. Mater. Interfaces*, 2019, **11**, 26830-26841.
6. C. Duan, D. Hook, Y. Chen, J. Tong and R. O'Hayre, *EES*, 2017, **10**, 176-182.
7. O. A. Aksan and N. Kizildag, *Energy Fuels*, 2025, **39**, 16505-16537.
8. H. Gu, M. Xu, Y. Song, C. Zhou, C. Su, W. Wang, R. Ran, W. Zhou and Z. Shao, *Compos. Pt. B-Eng.*, 2021, **213**, 108726.
9. Y. Chen, Y. Choi, S. Yoo, Y. Ding, R. Yan, K. Pei, C. Qu, L. Zhang, I. Chang, B. Zhao, Y. Zhang, H. Chen, Y. Chen, C. Yang, B. deGlee, R. Murphy, J. Liu and M. Liu, *Joule*, 2018, **2**, 938-949.
10. L. Troncoso, J. A. Alonso and A. Aguadero, *J. Mater. Chem. A*, 2015, **3**, 17797-17803.